

Time-resolved Langmuir probe diagnostics of high-power pulsed dc magnetron discharges during deposition of copper films

A.D. Pajdarová, J. Vlček, P. Kudláček, J. Lukáš, J. Musil

Department of Physics, University of West Bohemia, Univerzitní 22, 306 14 Plzeň, Czech Republic

Electron energy distribution functions and local plasma parameters were investigated at the substrate position (100mm from the target) by means of time-resolved Langmuir probe diagnostics during high-power pulsed dc magnetron sputtering of copper films. Very high plasma densities (up to $2 \times 10^{12} \text{cm}^{-3}$) were achieved at the voltage pulse repetition frequency $f_r = 1 \text{kHz}$, the pulse duration $t_l = 200 \mu\text{s}$, the argon pressure $p = 1 \text{Pa}$ and the average pulse current $I_{da} = 50 \text{A}$. At the same conditions, the kinetic temperature of electrons rose with an increasing power during a pulse. After an initial stage it was in the range 10500–12500K. Negative peaks of the floating potential were registered at the very beginning of the voltage pulse.

1. Introduction

High-power pulsed magnetron discharges for deposition of films are intensively investigated. A high power delivered to the magnetron target results in its intensive sputtering and effective ionization and excitation of sputtered atoms in the discharge. This makes it possible to form films under unique physical conditions [1-5].

2. Experimental set-up and procedure

A schematic diagram of the experimental device is shown in Fig. 1. All experiments were performed in a standard stainless steel vacuum chamber

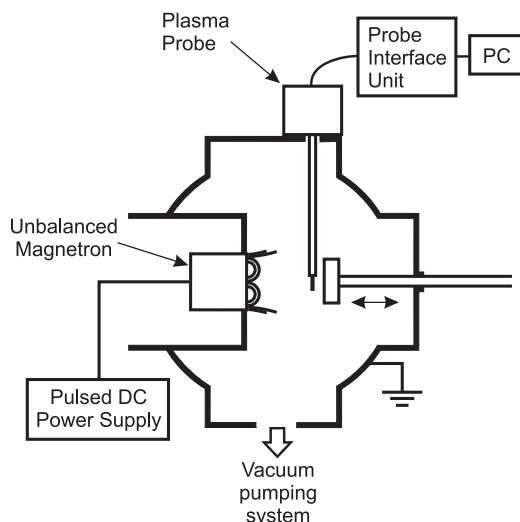


Fig. 1. Schematic diagram of the experimental set-up.

equipped with an unbalanced planar circular magnetron with a copper target (100mm in diameter). The magnetron was driven by a pulsed dc power supply (Rübig MP120) working in the frequency range from 0.5 to 50kHz with a maximum voltage and a maximum current of 1000V and 120A, respectively.

The time-resolved probe measurements were carried out using a Hiden ESPION system. A cylindrical probe tip (diameter 0.15mm and length

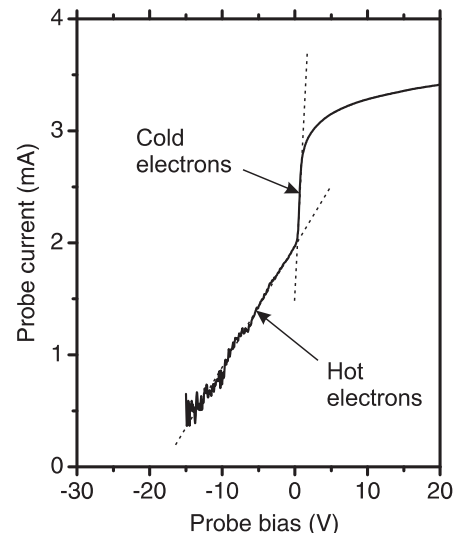


Fig. 2. Illustrative determination of the temperature of hot electrons and the temperature of cold electrons from a semi-logarithmic plot of the electron probe current.

10mm) was located in the center line of the discharge and positioned perpendicularly to the discharge axis. Target-to-tip distance was 100mm.

From the measured probe characteristics the electron energy distribution functions were determined using the Druyvesteyn formula [6]. The electron density n_e and the kinetic temperature of electrons T_e were calculated according to the formulas

$$n_e = \int_0^{\infty} f(E) dE$$

and

$$\bar{E} = \frac{3}{2}kT_e = \frac{1}{n_e} \int_0^{\infty} E f(E) dE,$$

where $f(E)$ is the electron energy distribution function, \bar{E} is the mean electron energy and k is the Boltzmann constant. The temperatures of hot and cold electrons were determined from the respective slopes of the semi-logarithmic plots of the electron probe current (see Fig. 2). The ion density n_i was calculated on the basis of the orbital motion limited theory [6] using the temperature of cold electrons. The plasma potential V_p was determined from the zero point of the second derivative of the electron probe current and the floating potential V_f from the zero value of the total probe current.

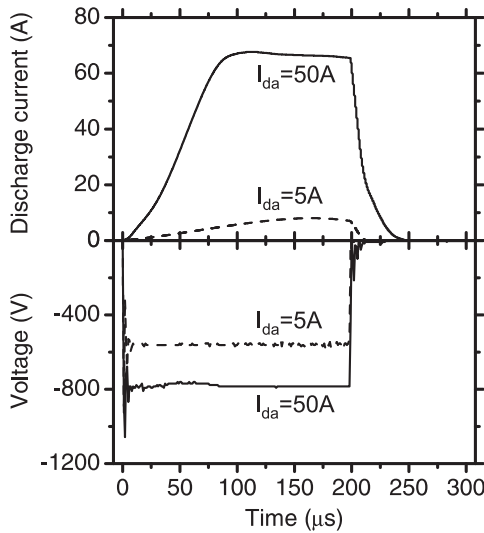


Fig. 3. Waveforms of the magnetron voltage and the discharge current.

3. Results

The results presented here were obtained at the voltage pulse repetition frequency $f_r = 1\text{kHz}$, the pulse duration $t_l = 200\mu\text{s}$, the argon pressure $p = 1\text{Pa}$ and the preset average pulse currents $I_{da} = 5$ and 50A . The average pulse current was calculated according to the formula

$$I_{da} = \frac{1}{t_l} \int_0^{t_l} I_d(t) dt,$$

where $I_d(t)$ is the discharge current.

Figure 3 shows waveforms of the magnetron voltage and the discharge current. The average power density during a pulse $P_{da} = U_d I_{da} / S$, where U_d is the magnetron voltage and S is a total target area (78.5cm^2), is 35W/cm^2 at $I_{da} = 5\text{A}$ and 500W/cm^2 at $I_{da} = 50\text{A}$.

The normalized electron energy distribution functions are depicted in Fig. 4 at the average pulse

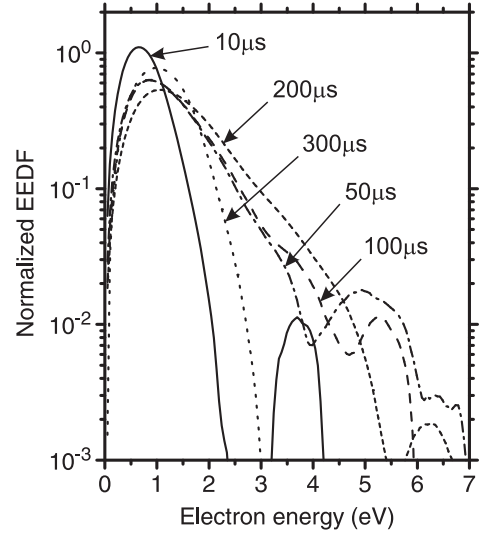


Fig. 4. Normalized electron energy distribution functions at selected times after a pulse initiation at the average pulse current $I_{da} = 50\text{A}$.

current $I_{da} = 50\text{A}$. The distributions with two energy groups of electrons are observed during a pulse, but the population of high-energy electrons is very low (approximately one hundred times lower than that of low-energy electrons).

Figure 5 shows time evolution of the kinetic temperature of electrons and the temperature of hot electrons during a pulse. At both the average currents, the kinetic temperature of electrons rises with an increasing power delivered to the plasma and after an initial stage it is in the range $10500\text{--}13000\text{K}$. The temperature of the weakly populated hot electrons decreases rapidly after the pulse initiation due to increasing density of copper atoms in the discharge and their effective ionization. At the average pulse current $I_{da} = 50\text{A}$ very high sputtering

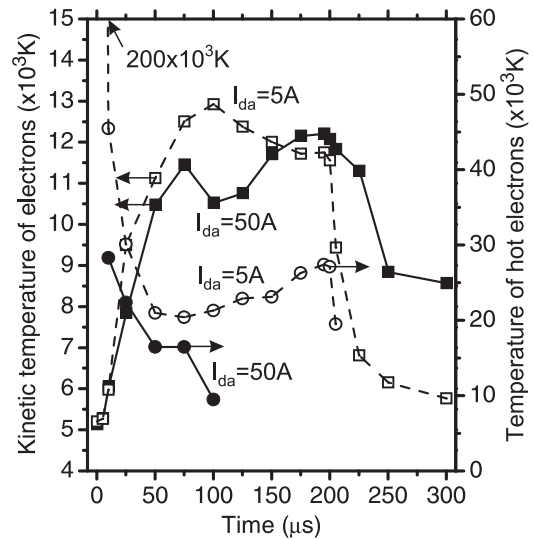


Fig. 5. Time evolutions of the kinetic temperature of electrons and the temperature of hot electrons.

rate of copper causes that the group of hot electrons coalesces with the bulk electrons after 100 μ s of a pulse (see the same values of temperatures).

Time evolutions of the electron and the ion densities are presented in Fig. 6. Very high plasma densities (up to $2 \times 10^{12} \text{ cm}^{-3}$) were achieved at the substrate position for $I_{da} = 50 \text{ A}$. Such high densities result in large fluxes of ions to the substrate. The waveforms of the plasma densities are delayed compared to those of the discharge current by approximately 50–60 μ s. The delay is caused by a transport of the sputtered copper atoms. Very good agreement between the ion densities and the electron densities was achieved particularly at the average pulse current $I_{da} = 50 \text{ A}$ except the very beginning of a pulse.

Figure 7 presents time evolutions of the plasma potential and the floating potential. The negative peaks of the floating potential at the very beginning of a pulse are caused by high-energy electrons, which are repelled from the target by a rapid drop of the target potential at the switching-on of the voltage pulse.

4. Acknowledgment

This work was supported by the Ministry of Education of the Czech Republic under Project No. MSM 4977751302 and ME 673.

5. References

- [1] K. Macák, V. Kouznetsov, J. Schneider, U. Helmersson, I. Petrov, J. Vac. Sci. Technol. A **18** (2000) 1533.
- [2] J. Musil, J. Leština, J. Vlček, T. Tölg, J. Vac. Sci. Technol. A **19** (2001) 420.
- [3] J. T. Gudmundsson, J. Alami, U. Helmersson, Appl. Phys. Lett. **78** (2001) 3427.
- [4] J. Vlček, A. D. Pajdarová, J. Musil, Contrib. Plasma Phys. **44** (2004) 437.
- [5] J. Vlček, P. Kudláček, K. Burcalová, J. Musil, J. Vac. Sci. Technol. A **25** (2007) 42.
- [6] J. D. Swift, M. J. R. Schwar: *Electrical Probes for Plasma Diagnostics*, Iliffe Books, London (1970).

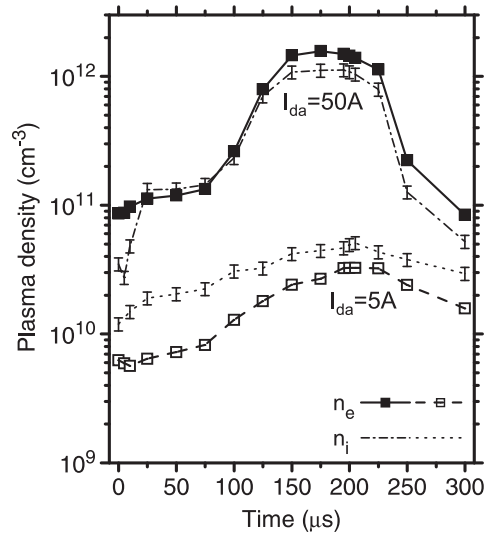


Fig. 6. Time evolutions of the electron densities and the ion densities.

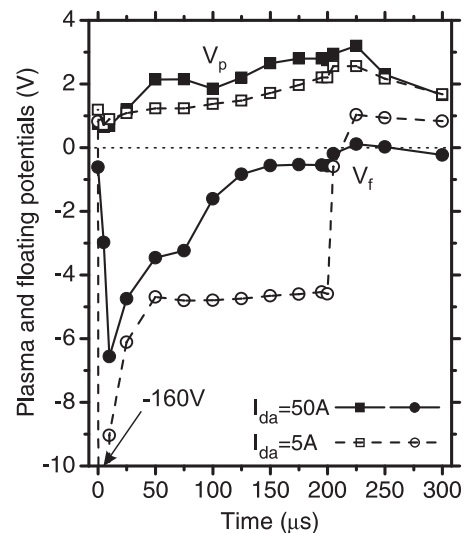


Fig. 7. Time evolutions of the plasma potential and the floating potential.